

INTEGRATED BUNDLE ADJUSTMENT WITH VARIANCE COMPONENT ESTIMATION – FUSION OF TERRESTRIAL LASER SCANNER DATA, PANORAMIC AND CENTRAL PERSPECTIVE IMAGE DATA

D. Schneider *, H.-G. Maas

Institute of Photogrammetry and Remote Sensing, Dresden University of Technology,
Helmholtzstraße 10, 01069 Dresden, Germany – (danilo.schneider, hans-gerd.maas)@tu-dresden.de

Commission V, WG V/3

KEY WORDS: Bundle adjustment, variance component estimation, laser scanner, camera, panorama, calibration

ABSTRACT:

Terrestrial laser scanners and digital cameras can be considered largely complementary in their properties. Several instruments combine a laser scanner and a camera, with the laserscanner providing geometry information and the camera supplying point of surface colour. These approaches of data fusion make sub-optimal use of the complementary properties of the two devices, as they assign a master-and-slave casting to laser scanner and camera. A thorough exploitation of the complementary characteristics of both types of sensors should start in 3D object coordinate determination with both devices mutually strengthening each other. For this purpose a bundle adjustment for the combined processing of terrestrial laser scanner data and central perspective or panoramic image data, based on an appropriate geometric model for each sensor, was developed. Since different types of observations have to be adjusted simultaneously, adequate weights have to be assigned to the measurements in a suitable stochastic model. For this purpose, a variance component estimation procedure was implemented, which allows to use the appropriate characteristics of the measurement data (e.g. lateral precision of image data, reliability of laser scanner range measurement), in order to determine 3D coordinates of object points. Finding optimal weights for the different groups of measurements leads to an improvement of the accuracy of 3D-coordinate determination. In addition, the integrated scanner and camera data processing scheme allows for the optimal calibration of the involved measurement devices (scanner+camera self-calibration). Moreover, it is possible to assess on the accuracy potential of the involved measurements. The presented paper describes the basic geometric models as well as the combined bundle adjustment with variance component estimation. First results, based on data in a 360° test field, are presented and analysed.

1. INTRODUCTION

Several software packages nowadays provide the possibility of combined processing of terrestrial laser scanner data and photogrammetric image data, since the combination of three-dimensional point clouds and images presents promising prospects due to their complementary characteristics. For this reason manufactures of terrestrial laser scanners also integrate digital cameras in their scanning hardware (Ullrich et. al., 2003; Mulsow et. al., 2004). In these integrated systems, the laser scanner usually represents the dominant device, while the image information is only used secondarily for the colouring of point clouds, texturizing of surfaces or to support the interpretation in interactive laser scanner data handling. Beyond this, the use of images for the automatic registration of laser scanner datasets was suggested in previous approaches (Al-Manasir & Fraser, 2006; Dold & Brenner, 2006), as well as the automatic generation of orthophotos on the basis of image and range data (Reulke, 2006).

The integrated analysis of terrestrial laser scanner data and photogrammetric image data provides a much larger potential (Jansa et. al., 2004; Wendt & Heipke, 2006). Using the complementary characteristics of both sensor types consistently in a combined adjustment, laser scanner and camera may mutually benefit from each other in the determination of object geometry and in calibration (Ullrich et. al., 2003).

In particular, high resolution cameras may be rather beneficial in a combined system, since the high angular accuracy of sub-pixel accuracy image measurements may help to improve the

lateral accuracy of laser scanners. Adapting to the operating mode of most laser scanners, which cover a 360° field of view, the use of panoramic cameras may be an interesting alternative to conventional central perspective cameras. Panoramic cameras often have a very high resolution and a large accuracy potential for the determination of 3D object coordinates (Luhmann & Tecklenburg, 2004; Schneider & Maas, 2005).

Based on the geometric models of laser scanner and camera, as well as a geometric model of panoramic cameras, which was developed at the Institute of Photogrammetry and Remote Sensing of the TU Dresden (Schneider & Maas, 2006), a combined bundle adjustment tool for the integrated processing of terrestrial laser scanner data, central perspective and panoramic image data was developed.

Since the procedure requires the simultaneous adjustment of different types of observations, it is necessary to assign adequate weights to the groups of measurements at the combined adjustment. These weights may be specified by the user, based on manufacturer specifications or practical experience. More rigorously, the weights can be determined automatically in the adjustment procedure by variance component estimation. Thus, the respective characteristics of the involved measurement devices will be optimally utilised, and an improvement of the adjustment results can be achieved (Klein, 2001; Sieg & Hirsch, 2000). Results of variance component estimation in a combined adjustment of laser scanner and image data are also presented in (Haring et. al., 2003).

* Corresponding author.

In this paper the implementation of a combined bundle adjustment with variance component estimation is described and analysed on the basis of multiple laser scans, central perspective and panoramic images in a 360° test field at TU Dresden.

2. GEOMETRIC MODELS

One precondition for the combined analysis of measurements from different devices (laser scanner, camera, panoramic camera) is the knowledge about the basic geometric models as well as their mathematical description. This allows for the calculation of object information (e.g. coordinates of object points) using different observations (range, angles, image coordinates) on the one hand and for the calibration of the involved measurement devices on the other hand, if the geometric models are extended by an appropriate set of additional parameters.

2.1 Central perspective and panoramic images

Cameras with area sensors comply with the known central perspective model (Figure 1). Mathematically this is described by the collinearity equations. Usually these equations are extended by correction terms, which contain additional parameters (Brown, 1971; El-Hakim, 1986) to compensate errors caused by lens distortion and other effects.

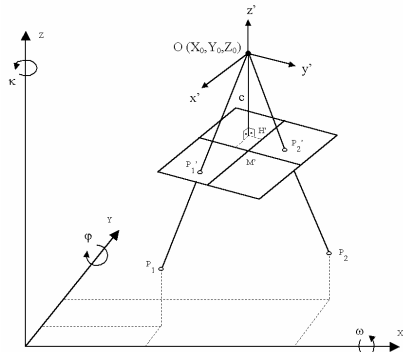


Figure 1. Central perspective camera model

Panoramic cameras are able to record a 360° horizontal field of view in one image, which is in particular beneficial for the recording of big interiors. Technically this is mostly realised by the rotation of a linear sensor. Panoramic cameras provide a very high resolution and accordingly a high accuracy potential. The panoramic camera model can be described by central perspective geometry only in one coordinate direction. The mapping process (Figure 2) can be represented by the projection onto a cylinder (Schneider & Maas, 2006; Amiri Parian, 2007).

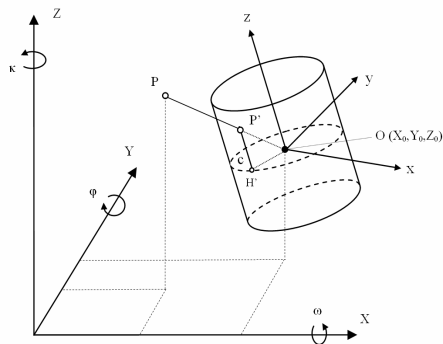


Figure 2. Panoramic camera model

The mathematical descriptions of the geometric models of central perspective and panoramic cameras (see Schneider & Maas, 2006 for the derivation) are:

$$x' = x_0' - \frac{c \cdot x}{z} + dx' \quad (1)$$

$$y' = y_0' - \frac{c \cdot y}{z} + dy'$$

$$x'_{pano} = x_0' - c \cdot \arctan\left(\frac{-y}{x}\right) + dx'_{pano} \quad (2)$$

$$y'_{pano} = y_0' - \frac{c \cdot z}{\sqrt{x^2 + y^2}} + dy'_{pano}$$

The transformation into a uniform coordinate system occurs by:

$$\begin{aligned} x &= r_{11}(X - X_0) + r_{21}(Y - Y_0) + r_{31}(Z - Z_0) \\ y &= r_{12}(X - X_0) + r_{22}(Y - Y_0) + r_{32}(Z - Z_0) \\ z &= r_{13}(X - X_0) + r_{23}(Y - Y_0) + r_{33}(Z - Z_0) \end{aligned} \quad (3)$$

where c = principal distance
 x', y' = image coordinates
 x_0', y_0' = principal point coordinates
 x'_{pano}, y'_{pano} = panoramic image coordinates
 X_0, Y_0, Z_0 = coordinates of projection center
 X, Y, Z = coordinates of object points
 r_{ij} = elements of rotation matrix
 x, y, z = coordinates of object points in the local camera coordinate system

The correction terms dx', dy' as well as dx'_{pano} and dy'_{pano} contain additional parameters for the compensation of systematic errors, which are caused by the physical characteristics of the cameras.

2.2 Laser scanner

Original measurement data of terrestrial laser scanners are spherical coordinates, i.e. range (D), horizontal (α) and vertical (β) angle. Therefore the geometric model can be described easily by the conversion of Cartesian into spherical coordinates (eq. 4). Applying equation (3), the local laser scanner coordinate system can be integrated into the uniform object coordinate system.

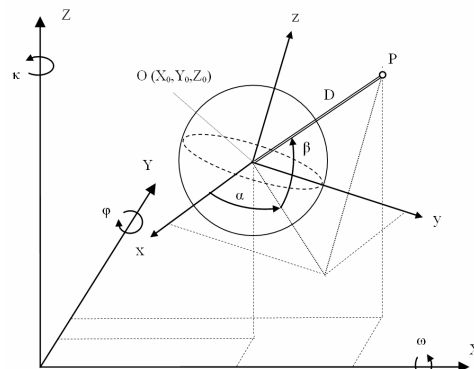


Figure 3. Laser scanner basic model

$$D = \sqrt{x^2 + y^2 + z^2} + dD \tag{4}$$

$$\alpha = \arctan\left(\frac{y}{x}\right) + d\alpha$$

$$\beta = \arctan\left(\frac{z}{\sqrt{x^2 + y^2}}\right) + d\beta$$

Analogous to the camera model, additional parameters can be considered within the correction terms dD , $d\alpha$ and $d\beta$ as an extension of the geometric model of terrestrial laser scanners. This allows for the compensation of systematic deviations from the basic model and thus for the calibration of laser scanners.

However, the calibration of terrestrial laser scanners is complicated by the fact that the manufacturers already implement geometric corrections inside the scanner, whose underlying model equations are mostly not known. Subsequently, significant systematic effects can often not be detected in the residuals of the observations. Therefore only a distance offset (k_0) and scale (k_s) parameter were used in the geometric model (eq. 5) so far, but no corrections of the horizontal and vertical angle were considered.

$$dD = k_s \cdot D + k_0 \tag{5}$$

3. INTEGRATED BUNDLE ADJUSTMENT

Bundle adjustment allows for the orientation of an arbitrary number of images, using the image coordinates of object points as observations. The results of the calculation are the orientation parameters of the images, the 3D coordinates of object points and possibly camera self-calibration parameters. Extending this approach to the combined bundle adjustment means the integration of all laser scans, central perspective and panoramic images of each involved measurement device (scanner, camera, panoramic camera). The calculation follows the geometric constraint that all corresponding rays between object point and the instrument should intersect in their corresponding object point.

The spherical coordinates of object points measured with a laser scanner as well as the image coordinates of a camera respectively a panoramic camera are introduced as observations in one combined coefficient matrix. Figure 4 shows a synthetic example of the structure of a design matrix.

The calculation is performed as a least squares adjustment. The results are the coordinates of object points, the position and orientation of each involved scan and image, the calibration parameters of the measurement devices as well as statistical values for the assessment of accuracies and correlations.

For the calculation of the bundle adjustment a software was developed at the Institute of Photogrammetry and Remote Sensing of TU Dresden, which also allows exporting a protocol and a visualisation file. All settings are displayed in a graphical user interface (Figure 5) and can be changed if necessary. In order to detect and to eliminate outliers a data-snooping procedure following (Baarda, 1968) is applied.

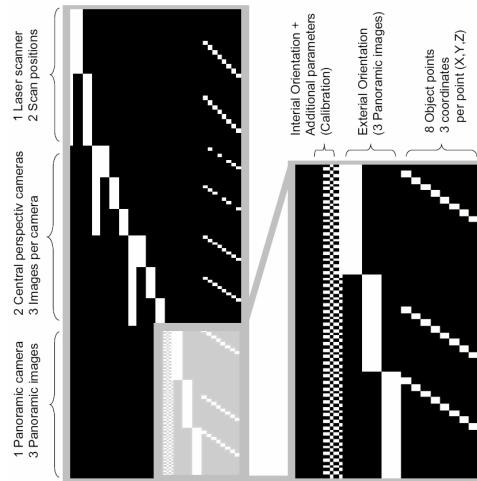


Figure 4. Structure of design matrix (example)

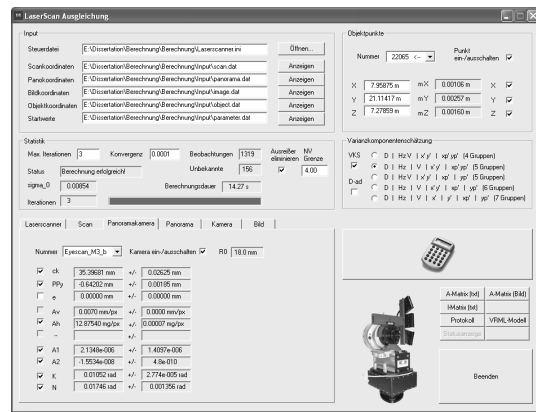


Figure 5. User interface of combined adjustment

Within a courtyard at TU Dresden a 360° test field with ca. 100 retroreflective targets (circles with 5 cm diameter) was installed to practically verify the combined bundle adjustment. The dimensions of this courtyard are 45 m × 45 m, the surrounding façades are 20 m high. The scanner used in the practical tests was a Riegl LMS-Z420i, whose operating software allows for the automatic determination of the centre of retroreflective targets applying a centroid operator to the intensity image. Furthermore multiple panoramas were captured with the KST Eyescan M3metric panoramic camera (Schneider & Maas, 2006), as well as a large number of images from digital SLR cameras Kodak DCS 14n and Nikon D100. The target image coordinates were determined using centroid and ellipse operators. In the following, the results of processing the data of several different sensor combinations in the test field will be shown.

3.1 Example 1

This example shows the calculation of the 3D coordinates of 10 object points of a façade of the test field. Two laser scanner positions and two panoramic camera positions were stepwise introduced into the combined bundle adjustment in different constellations, and the standard deviation of the estimated object coordinates were analysed. Figure 6 shows the used configuration schematically.

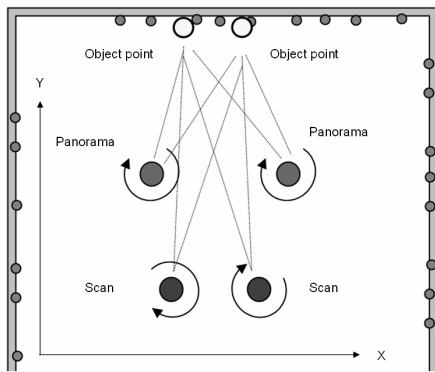


Figure 6. Imaging configuration 1 (schema)

Using only 2 panoramic images for the bundle adjustment, the precision of the resulting object coordinates (mainly in imaging direction Y) is worse than the precision obtained from one laser scan (see Table 1). This can be explained by poor intersection geometry of the used panorama positions. Furthermore the potential of the high-resolution panoramic camera could not be exploited, since the retroreflective targets could not be illuminated properly and the subpixel potential of the image analysis operators could not be used to full extent. Nevertheless, the combination of both devices (at least one scan and one panoramic image) leads to a significant precision improvement.

| Number of scans | Number of panoramas | $\hat{\sigma}_D$ (mm) | $\hat{\sigma}_{\alpha,\beta}$ (mgon) | $\hat{\sigma}_{xp,yp}$ (pixel) | RMS_X (mm) | RMS_Y (mm) | RMS_Z (mm) |
|-----------------|---------------------|-----------------------|--------------------------------------|--------------------------------|--------------|--------------|--------------|
| 1 | – | 7.45 | 4.92 | – | 2.82 | 6.83 | 3.36 |
| 1* | – | 5.56 | 4.91 | – | 2.55 | 5.22 | 2.93 |
| – | 2 | – | – | 0.55 | 4.18 | 14.15 | 4.99 |
| 1 | 1 | 5.56 | 4.85 | 0.59 | 2.25 | 5.07 | 2.61 |
| 1 | 2 | 5.84 | 4.88 | 0.62 | 1.96 | 4.81 | 2.51 |
| 2 | – | 6.87 | 6.30 | – | 2.53 | 4.83 | 2.95 |
| 2 | 1 | 6.48 | 5.65 | 0.68 | 2.12 | 4.47 | 2.51 |
| 2 | 2 | 6.21 | 5.42 | 0.65 | 1.91 | 4.33 | 1.88 |

Table 1. Example 1: Calculation results of different configurations (calculated with variance component estimation – see chapter 4)

While the laser scanner measurements improve the accuracy in depth direction, the image observations of the panoramic camera ensure a better precision in lateral coordinate direction. If further scans or images are added, the RMS of the standard deviations of object point coordinates can be minimized accordingly, as long as good intersection angles are maintained.

3.2 Example 2

The next example analyses the precision improvement achieved by the use of additional central perspective images. For this purpose 4 laser scans, 5 panoramic images and a total of 62 images with the Kodak DSC 14n were recorded (Figure 7 shows a reduced number of camera positions). The recording configuration was chosen with regard to good intersection geometry. Furthermore additional images with a camera Nikon D100, which was mounted on top of the Riegl laser scanner,

were captured and included into the calculation. Figure 8 shows the devices involved into this calculation example.

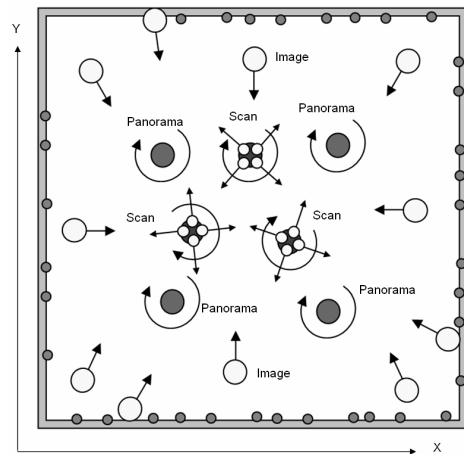


Figure 7. Imaging configuration 2 (schema)



Figure 8. Combined devices (Riegl laser scanner LMS-Z420i, panoramic camera Eyescan M3, Kodak 14n, Nikon D100)

The results of this example show, that the integration of additional panoramic or central perspective images has the potential to improve the accuracy of the calculated results in general. This can be realized in practice, if the user takes additional images while the laser scan runs automatically, subsequently feeding the images into the calculation process. Similarly the images of a camera mounted on top of a laser scanner respectively a camera integrated within the laser scanner hardware can contribute to increase the accuracy. The large number of additional images of the last calculation example in Table 2 may be unrealistic for practical use, but shows the accuracy potential of the combined bundle adjustment.

4. VARIANCE COMPONENT ESTIMATION

The combined bundle adjustment uses different types of observations simultaneously in order to estimate the unknown parameters. For this reason it is necessary to assign suitable weights to the different groups of observations (image coordinates in central perspective and panoramic images, range measurement and angle measurements of the laser scanner). The definition of weights can be performed in terms of fix values, in case of known a-priori standard deviations of the measurements (e.g. specifications of the manufacturer) or if experience values are available. However, the information content of the observations is not fully exploited in this case.

* with consideration of scale and offset, according to eq. (4)

| Number of scans | Number of panoramas | Number of central perspective images | | Unknown object points | $\hat{\sigma}_D$ (mm) | $\hat{\sigma}_{\alpha,\beta}$ mgon | $\hat{\sigma}_{x_p',y_p'}$ (pixel) | $\hat{\sigma}_{x',y'}$ (pixel) | RMS _X (mm) | RMS _Y (mm) | RMS _Z (mm) |
|-----------------|---------------------|--------------------------------------|-------|-----------------------|-----------------------|------------------------------------|------------------------------------|--------------------------------|-----------------------|-----------------------|-----------------------|
| | | Kodak | Nikon | | | | | | | | |
| 3 | — | — | — | 35 | 5.22 | 5.62 | — | — | 2.28 | 2.19 | 1.75 |
| 3 | 4 | — | — | 35 | 5.19 | 5.45 | 0.59 | — | 1.89 | 1.67 | 1.26 |
| 3 | — | 18 | — | 35 | 5.27 | 5.76 | — | 0.30 | 1.86 | 2.08 | 1.55 |
| 3 | — | — | 18 | 35 | 5.19 | 5.70 | — | 0.18 | 1.81 | 2.04 | 1.52 |
| 3 | 4 | 18 | — | 35 | 5.23 | 5.55 | 0.59 | 0.29 | 1.51 | 1.62 | 1.12 |
| 3 | 4 | — | 18 | 35 | 5.20 | 5.63 | 0.60 | 0.19 | 1.50 | 1.61 | 1.12 |
| 3 | — | 18 | 18 | 35 | 5.24 | 5.79 | — | 0.24 | 1.80 | 2.03 | 1.49 |
| 4 | 5 | 62 | 42 | 8 | 5.59 | 5.91 | 0.63 | 0.25 | 0.49 | 1.12 | 0.60 |

Table 2. Example 2: Calculation results of different configurations (calculated with variance component estimation – see chapter 4)

Using the variance component estimation procedure (VCE) it is possible to estimate optimal weights for each group of observations as well as standard deviations of the observations in the course of the bundle adjustment. This allows for the qualification of each group of measurement on the one hand and for an improvement of the adjustment results on the other hand, since the individual characteristics of the involved measurement devices can be optimally utilised (Klein, 2001; Sieg & Hirsch, 2000). By separating the horizontal and vertical angle measurement of the laser scanner as well as the horizontal and vertical image coordinates of the panoramic camera into different groups of observation, it becomes possible to draw conclusions on the characteristics of each instrument.

Furthermore, also cameras or laser scanners with different accuracies can be considered simultaneously.

The weights p_i of the observations are determined by the ratio of the variance of the unit weight σ_0^2 and the variance of the observations σ_i^2 , which can be derived from manufacturer's data or from empirical values. A constant value will be set for σ_0 (e.g. 0.01 in the presented examples). Subsequently, the standard deviation of unit weight $\hat{\sigma}_0$ shows if the a-priori standard deviations of the observations were defined too pessimistic ($\hat{\sigma}_0 < \sigma_0$) or too optimistic ($\hat{\sigma}_0 > \sigma_0$).

| Calculation example | Weighting | $\hat{\sigma}_0$ | RMS _X (mm) | RMS _Y (mm) | RMS _Z (mm) | RMS _{XYZ} (mm) |
|---------------------|---|------------------|-----------------------|-----------------------|-----------------------|-------------------------|
| 1 | Balanced (but too pessimistic overall) | 0.00573 | 1.58 | 1.71 | 1.16 | 2.60 |
| 2 | Balanced (but too optimistic overall) | 0.02296 | 1.63 | 1.83 | 1.15 | 2.71 |
| 3 | Balanced and realistic constant weights | 0.01046 | 1.59 | 1.74 | 1.19 | 2.64 |
| 4 | Unbalanced (range too optimistic) | 0.01309 | 1.78 | 1.78 | 2.03 | 3.23 |
| 5 | Unbalanced (angles too optimistic) | 0.01479 | 2.03 | 2.62 | 1.33 | 3.57 |
| 6 | Unbalanced (panoramic coordinates too optimistic) | 0.01320 | 2.12 | 2.31 | 1.32 | 3.40 |
| 7 | Unbalanced (central perspective coordinates too optimistic) | 0.01061 | 2.68 | 3.05 | 1.94 | 4.50 |
| 8 | VCE, 4 groups: D α, β x_p', y_p' x', y' | 0.01000 | 1.51 | 1.64 | 1.13 | 2.50 |
| 9 | VCE, 5 groups: D α β x_p', y_p' x', y' | 0.01000 | 1.56 | 1.68 | 1.04 | 2.52 |
| 10 | VCE, 5 groups: D α, β x_p' y_p' x', y' | 0.01000 | 1.47 | 1.60 | 1.16 | 2.46 |
| 11 | VCE, 6 groups: D α β x_p' y_p' x', y' | 0.01000 | 1.52 | 1.63 | 1.05 | 2.46 |
| 12 | VCE, 7 groups: D α β x_p' y_p' x' y' | 0.01000 | 1.52 | 1.63 | 1.05 | 2.46 |

Table 3. Combined bundle adjustment with different stochastic models

| Standard deviation of observations | too optimistic/ too pessimistic | | | Unbalanced weights | | | | Variance component estimation | | | | |
|------------------------------------|------------------------------------|---------------|---------------|---------------------|----------------|----------------|----------------|-------------------------------|----------------|----------------|----------------|----------------|
| | 1 | 2 | 3 | 4 | 5 | 6 | 7 | 8 | 9 | 10 | 11 | 12 |
| Range (mm) | (10.0) 5.73 | (3.0) 6.89 | (5.3) 5.54 | (2.0) 2.0 | (10.0) 14.8 | (10.0) 13.2 | (10.0) 10.6 | (7.5) 5.23 | (7.5) 5.21 | (7.5) 5.24 | (7.5) 5.22 | (7.5) 5.23 |
| Horizontal angle (mgon) | | | | | | | | | (10.0) 4.23 | | (10.0) 4.21 | (10.0) 4.21 |
| Vertical angle (mgon) | | | | | | | | | (10.0) 6.61 | (10.0) 5.58 | (10.0) 6.64 | (10.0) 6.64 |
| Panoramic x_p' (pixel) | | | | | | | | | (0.5) 0.52 | (0.5) 0.52 | (0.5) 0.52 | (0.5) 0.52 |
| Panoramic y_p' (pixel) | | | | | | | | | 0.60 | 0.60 | 0.66 | 0.66 |
| Central perspective x' | | | | | | | | | | | | (0.2) 0.26 |
| Central perspective y' | | | | | | | | | 0.24 | 0.24 | 0.24 | (0.2) 0.23 |

Table 4. Combined bundle adjustment with different stochastic models (in brackets: standard deviation for the a-priori definition of observation weights; hereunder: estimated a-priori standard deviations of observations)

If observations of the same type have to be processed, the variance-covariance matrix Σ is calculated as product of σ_0^2 and the cofactor matrix Q . In case of a combined adjustment of different observation groups the matrix Σ will be split into components $\Sigma_i = \sigma_i^2 Q_i$. The factors σ_i^2 are the variance components to be estimated which represent the a-priori measurement inaccuracies of each observation group. The calculation is carried out as described in (Koch, 1997; Sieg & Hirsch, 2000).

Table 3 and 4 show the results of 12 different practical examples. The weighting of examples 1 and 2 was balanced but too pessimistic respectively too optimistic. For example 3 well balanced and realistic weights were used as constant values. Examples 4-7 started with unfavourable unbalanced observation weights, examples 8-12 were calculated with integrated variance component estimation, each with different constellations (compare table 4) of observation groups.

Generally it is noticeable that the variance component estimation has the potential to contribute to the improvement of the accuracy, in particular, if the precision of the involved instruments is not sufficiently well known a-priori (see table 3). Table 4 demonstrates the capability of the calculation with variance component estimation to estimate the precision of the involved groups of measurements – widely independent from the definition of a-priori approximate weights.

The values in brackets served for the definition of weights for each observation. The values below are the estimated a-priori standard deviations as results of the bundle adjustment. This value is better than the value in brackets if the weighting was too pessimistic and worse if the weighting was too optimistic. This is in particular noticeable with example 1 and 2. In Examples 4-7 only one group of observations started with too optimistic standard deviations which lead to overemphasized weights for this group of observations (in table 4 highlighted with boldface). Anyway, the adjustment results change for the worse in these cases (see RMS of object coordinates in table 3). The variance component estimation (examples 8-12) results in balanced weights and therefore in optimal adjustment outcomes. The values in brackets in table 4 serve in these cases only for the definition of a-priori approximate weights. The values below are the variance components estimated within the adjustment with VCE. These variance components give realistic information about the precision of each observation group.

Furthermore, it is even possible to draw conclusions on differences of the horizontal and vertical angle precision of the laser scanner, as well as on differences in the horizontal and vertical image coordinate accuracy, in particular for panoramic cameras. In future the separation into more observation groups will be analysed (e.g. by use of different cameras or scans with different resolution, separation in constant and distance-dependent variance components). In addition, the implementation and assessment of a free net adjustment (without datum points) with variance component estimation is planned. In order to assess the accuracy more realistically, independent test measurements respectively a comparison of the estimated object point coordinates with known object coordinates, measured with a higher accuracy, will be performed.

5. REFERENCES

- Al-Manasir, K. & Fraser, C., 2006: Automatic registration of terrestrial laserscanner data via imagery. *ISPRS Archives*. Vol. XXXVI, Part 5.
- Amiri Parian, J., 2007: Sensor modelling, terrestrial panoramic camera calibration and close-range photogrammetric network analysis. *Dissertation ETH Zürich*.
- Baarda, W., 1968: A testing procedure for use in geodetic networks. *Netherlands Geodetic Commission*, Vol. 2 (5), Delft.
- Brown, D., 1971: Close-Range Camera Calibration. *Photogrammetric Engineering*, Vol. 37, No. 8.
- Dold, C. & Brenner, K., 2006: Registration of terrestrial laser scanning data using planar patches and image data. *ISPRS Archives*. Vol. XXXVI, Part 5.
- El-Hakim, S.F., 1986: Real-Time Image Meteorology with CCD cameras. *Photogrammetric Engineering and Remote Sensing*, Vol. 52, No. 11, pp. 1757-1766
- Haring, A.; Briese, M.; Pfeifer, N., 2003: Modellierung terrestrischer Laserscanner-Daten am Beispiel der Marc-Anton-Plastik. *Österreichische Zeitschrift für Vermessung und Geoinformation (VGI)*, 91. Jahrgang (2003), 4: 288-296.
- Jansa, J.; Studnicka, N.; Forkert, G.; Haring, A.; Kager, H., 2004: Terrestrial laserscanning and photogrammetry – acquisition techniques complementing one another. *ISPRS Archives*. Vol. XXXV, Part B5.
- Klein, B., 2001: Untersuchungen zur Feldprüfung geodätischer Instrumente mittels Varianzkomponentenschätzung. *Diplomarbeit, Technische Universität Darmstadt*, unpublished.
- Koch, K.-R., 1997: *Parameterschätzung und Hypothesentests in linearen Modellen*. Dümmler Verlag, Bonn, 3. Auflage.
- Luhmann, T. & Tecklenburg, W., 2004: 3-D object reconstruction from multiple-station panorama imagery. *ISPRS Archives*. Vol. XXXIV, 5/W16.
- Mulsow, C.; Schneider, D.; Ullrich, A.; Studnicka, N., 2004: Untersuchungen zur Genauigkeit eines integrierten terrestrischen Laserscanner-Kamerasystems. *Beiträge der Oldenburger 3D-Tage 2004*: 108-113, Herbert Wichmann Verlag, Heidelberg.
- Reulke, R., 2006: Combination of distance data with high resolution images. *Image Engineering and Vision Metrology, ISPRS Archives*. Vol. XXXVI, Part 5.
- Schneider, D. & Maas, H.-G., 2005: Combined bundle adjustment of panoramic and central perspective images. *ISPRS Archives*. Vol. XXXVI, Part 5/W8.
- Schneider, D. & Maas, H.-G., 2006: A geometric model for linear-array-based terrestrial panoramic cameras. *The Photogrammetric Record*, 21(115): 198-210, Blackwell Publishing Ltd., Oxford, UK.
- Sieg, D. & Hirsch, M., 2000: Varianzkomponentenschätzung in ingenieurgeodätischen Netzen; Teil 1: Theorie. *Allgemeine Vermessungsnachrichten*, 3/2000: 82-90.
- Ullrich, A.; Schwarz, R.; Kager, H., 2003: Using hybrid multi-station adjustment for an integrated camera laser-scanner system. *Optical 3-D Measurement Techniques VI*, Vol. 1 (2003), 298-305.
- Wendt, A. & Heipke, C., 2006: Simultaneous orientation of brightness, range and intensity images. *ISPRS Archives*. Vol. XXXVI, Part 5.